Vol. 04, Iss. 3 (2026) 1-7, DOI: 10.61552/JME.2026.03.003

JME

Journal of Materials and Engineering

www.jme.aspur.rs

Research article

Temperature-Driven Carbonation Of Steel Slag For Carbon Capture And Storage (CCS) Applications

Umi Rukiah Abdullah[a], Adibah Abd Aziz[a], Faradiella Mohd Kusin[a,b,*]

[a]*Socio-Environmental Waste Solution Hub (SEWaSH), Faculty of Forestry and Environment, Universiti Putra Malaysia, 43400 UPM Serdang, Selangor, Malaysia,*
[b]*Institute of Tropical Forestry and Forest Products (INTROP), Universiti Putra Malaysia, 43400 UPM Serdang, Selangor, Malaysia.*

Keywords:

CCUS
Carbon utilization
Industrial waste
Mineral carbonation
Climate action

* Corresponding author:

Faradiella Mohd Kusin
E-mail: faradiella@upm.edu.my

Received: 17 July 2025
Revised: 5 August 2025
Accepted: 12 September 2025

ABSTRACT

This study investigates the effect of temperature on the carbonation efficiency, mineral transformation, and microstructural changes of steel slag to enhance its potential for carbon capture and storage. Carbonation experiments were conducted at 25°C, 40°C, and 80°C. Results show that calcium carbonation efficiency increased with temperature, peaking at 81.62% at 40°C before slightly declining at 80°C. XRD analysis revealed dominant calcite formation at all temperatures, with the highest siderite content observed at 40°C. SEM and EDX analyses confirmed more uniform carbonate layers and reduced porosity at elevated temperatures, particularly at 80°C. TGA/DTG analysis supported these findings, showing higher CO_2 retention and distinct thermal decomposition behavior in carbonated samples. Overall, 40°C was identified as the optimal temperature for efficient and energy-effective carbonation. The study highlights steel slag's potential as a low-cost, reactive material for CO_2 mineralization under moderate temperature conditions.

1. INTRODUCTION

In response to the growing threat of climate change, carbon capture, utilization, and sequestration (CCUS) has emerged as a critical technology aimed at reducing greenhouse gas emissions, particularly carbon dioxide (CO_2). This process involves capturing CO_2 from industrial sources or directly from the atmosphere, utilizing it for various applications, and storing it to prevent its release into the atmosphere. The carbon capture component is typically achieved through methods such as chemical absorption, physical adsorption, and membrane separation, with chemical absorption, which often uses amine-based solvents, being the most widely adopted technique [1,2]. However, the commercial viability of CO_2 capture technologies faces significant challenges, including high capital costs, energy requirements for CO_2 desorption, and solvent losses [1].

Once captured, CO_2 can be utilized in a variety of applications, such as enhanced oil recovery, the production of fine chemicals, pharmaceuticals, and polymers. The utilization of CO_2 not only creates valuable products but also offers economic benefits by reducing the need for raw materials from natural sources [3,4]. The sequestration aspect of CCUS focuses on safely storing CO_2 to prevent its release into the atmosphere. Common sequestration methods include geological sequestration, which involves injecting CO_2 into depleted oil and gas fields, saline aquifers, and unmineable coal seams. In recent years, ocean sequestration and mineral carbonation have also emerged as promising methods for long-term CO_2. The goal of geological sequestration is to permanently convert CO_2 into stable mineral forms, thereby reducing the need for ongoing monitoring and ensuring the safe storage of CO_2 for extended periods [5].

In this context, mineral carbonation represents a particularly promising aspect of CCU (carbon capture and utilization). Unlike traditional sequestration methods that focus on storing CO_2, mineral carbonation offers a pathway for permanently storing CO_2 in stable mineral forms, effectively integrating both carbon capture and utilization [6]. This process involves the conversion of CO_2 into solid carbonates by reacting it with metal oxides, such as those found in steel slag, offering a dual benefit of CO_2 sequestration and the production of valuable by-products. Mineral carbonation not only ensures long-term CO_2 storage but also contributes to the creation of supplementary cementitious materials (SCMs), reducing the need for natural minerals and thereby supporting a more sustainable construction industry. This integration of mineral carbonation into CCU aligns with the broader goal of achieving a circular carbon economy, where CO_2 is continuously captured, utilized, and stored in a way that mitigates climate change while creating economic value [1,3,4]. Therefore, mineral carbonation stands out as an ideal approach in the CCUS landscape, offering a permanent and environmentally safe solution for CO_2 storage while contributing to green innovation and the development of new markets for CO_2-derived products.

2. METHODOLOGY

2.1 Mineral carbonation experiment

An mineral carbonation experiments was carried out under identified conditions with sequential steps that include cation extraction, pH adjustment, CO_2 dissolution, and carbonate precipitation. Hydrochloric acid (HCl), was used as an extractant, with a 1.5 M concentration and a solid-liquid ratio of 1:10. This was based on the trial experiment, to determine the optimal conditions for the leaching phase [7]. The particle sizes of steel slag were less than 0.3 µm, which is regarded as fine particles [8]. Following the leaching procedure, the sample was filtered to eliminate any remaining particles and contaminants from the solution. pH was then adjusted to ~12 by adding a 2 M of sodium hydroxide (NaOH). The steel slag sample underwent carbonation in a carbonation reactor under specific temperature, CO_2 pressure, and reaction time. A stainless-steel carbonation reactor with a working capacity of 250 mL was used. The carbonated slurry was collected after the carbonation has ceased, and was then filtered and air dried for further characterization analysis. To investigate the effect of varying temperature conditions, experiments were conducted at ambient pressure (1 bar) and reaction time of 30 minutes. The carbonation efficiency (%) was determined by calculating the weight loss obtained from thermogravimetric, TGA analysis. Equations (1) and (2) show that x is the oxide element, i.e., Ca or Fe, MW is the molecular weight, and ΔW is the sample weight loss from TGA analysis.

$$\text{Carbonation efficiency (\%)} = \frac{\text{X mass in XCO}_3}{\text{X total in feeding material}} \times 100 \qquad (1)$$

$$\text{X mass in XCO}_3 = \Delta\text{W (\%)} \times \frac{\text{Mw}_\text{X}}{\text{MwCO}_2} \qquad (2)$$

2.2. Sample characterization analysis

Samples of raw and carbonated steel slag were subjected to characterization analysis including chemical, morphological and mineralogical analyses. The steel slag samples were analyzed using X-ray diffraction (XRD), to identify the crystalline phase, with a Bruker-AXS D8 Advanced diffractometer. Scans were taken at 1°/min rate (0.025° step size) and counting for 0.2 s per step over the 5–50° scattering angle range. Integrated intensity of peak areas was determined using Diffrac AT EVA software (v.9.0) to obtain the mineral composition and crystalline phases of the samples [9]. The d-spacing was identified using OriginPro 2024b software (Originlab Corporation, Northampton, UK). Surface morphological structure of the steel slag sample was observed under scanning electron microscopy (SEM) at the magnification of x10,000. The SEM instrument (model JEOL JSM-6400) is equipped with energy dispersive X-ray (EDX) to quantify (in %) the elemental composition of the raw and carbonated samples. The carbonate formation of raw and carbonated steel slag was determined from the thermogravimetric analysis (TGA) using a TGA instrument (model Mettler Toledo TGA/DSC 3^+, Switzerland). The TGA was used to determine the weight loss of samples subjected to 30°C to 1000°C heating. The decomposition of steel slag samples was presumed to be associated to the decarbonization of carbonate species under specific temperature ranges.

3. RESULTS AND DISCUSSION

3.1. Carbonation efficiency

Figure 1 shows the Ca and Fe carbonation efficiency of the steel slag samples across different temperatures. The results indicate that Ca carbonation efficiency increases with temperature up to 40°C (69.43% at 25°C to 81.62% at 40°C) but slightly decreases at 80°C (80.80%). On the other hand, Fe carbonation efficiency shows some variation, ranging from 11.74% at 25°C to 12.81% at 40°C and 11.63% at 80°C. This trend shows that increasing the temperature at the start of the carbonation reaction accelerates the surface kinetics and improves reactive element dissolution. However, beyond a certain temperature, the combined effects of CO_2 concentration and other factors influence the diffusion rate of CO_2 into the material, potentially limiting further carbonation [10]. It can be seen that optimal carbonation temperature varies according to feedstock properties and experimental conditions. Varying temperatures have minimal impact on the carbonation efficiency of $CaCO_3$ and $FeCO_3$ observed between 25-80°C. Nonetheless, 40°C appears to be the most feasible operating temperature, as it provides a slightly higher carbonation efficiency comparable to that at 80°C, while being less energy intensive. This makes the carbonation process more attractive for practical applications in carbon capture and storage.

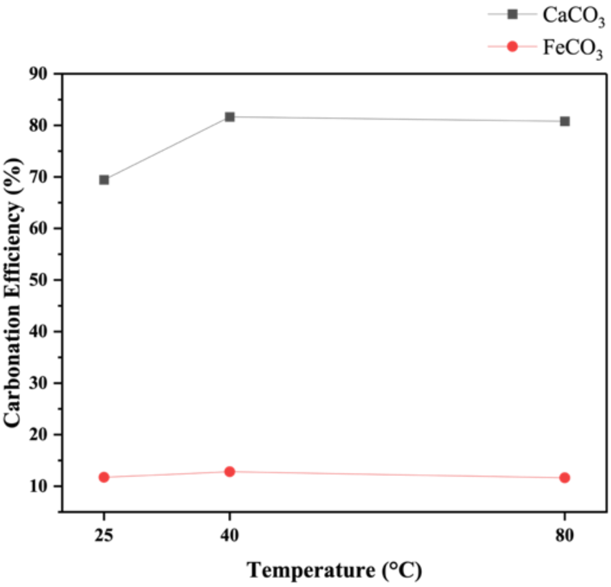

Fig. 1. Carbonation efficiency (%) at different temperatures (25°C, 40°C and 80°C) for $CaCO_3$ and $FeCO_3$.

3.2. Mineral phase transformation

Figure 2 shows the XRD patterns of carbonated samples at various temperatures (25°C, 40°C, and 80°C), indicating the difference in mineral phases formed throughout the carbonation process. At 25°C, calcite ($CaCO_3$) represents 61.1% of the mineral phases, with smaller amounts of dolomite ($CaMg(CO_3)_2$, 3.1%), siderite (FeCO3, 5.4%), and a significant amount of halite (30.4%). The high percentage of halite is likely due to the use of HCl and NaOH in the experiment. The high percentage of calcite suggests that, at ambient temperature, carbonation mostly takes place at the surface. Small amounts of siderite and dolomite, however, indicate that carbonation only occurs to specific mineral phases, most likely because of slower reaction rate at this lower temperature. The percentage of siderite ($FeCO_3$) increases significantly to 29.2% when the temperature is raised to 40°C, indicating that siderite formation is encouraged by higher temperatures. The concentration of calcite reduces slightly to 57.2%. This shift suggests that 40°C is more favorable to siderite production, probably due to higher Fe reactivity at this intermediate temperature. At 80°C, the calcite concentration rises to 69.4%, suggesting that higher temperatures can speed up the carbonation process for calcium-bearing phases, allowing higher amount of $CaCO_3$. Although siderite development is less favored than calcite at this temperature, the proportion of siderite (9.8%) is still higher than at 25°C but lower than at 40°C, suggesting that higher temperatures encourage the stability of both calcite and siderite. These findings show that higher temperatures (80°C) strongly promote calcite formation, which promotes carbonation efficiency for calcium-rich phases. In contrast, a moderate temperature (40°C) produces a greater variety of carbonates, including siderite. This supports previous research by [11], which suggests that an ideal temperature exists where surface carbonation is enhanced without slowing CO_2 diffusion, thereby improving the carbon capture potential of steel slag.

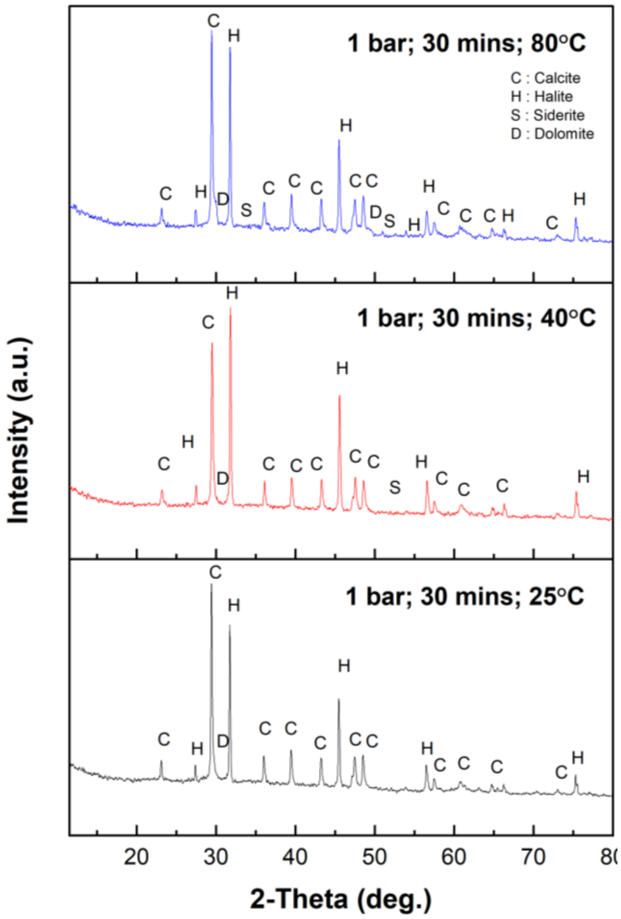

Fig. 2. XRD diffractogram of steel slag illustrating the mineral phases identified for the specified temperatures at ambient pressure (1 bar) and reaction time (30 mins).

3.3. Carbonate microstructure

The SEM analysis of carbonated samples are shown in Figure 3. The microstructure is heterogeneous at 25°C (Figure 3a), with agglomerated particles that have angular and rough surfaces. The sample has both amorphous and crystalline textures, with flake-like structures and compacted sections indicating lacking carbonation. Although the surface shows uneven coverage, small grain-like deposits are visible, likely representing the early stages of calcium carbonate ($CaCO_3$) formation. Visible fractured edges suggest that carbonation at this temperature is inefficient, likely due to volume changes during the reaction. This results in limited carbonation and uneven distribution of carbonate products. These observations suggest that higher temperatures could improve carbonation efficiency and uniformity, even with a constant reaction time [11]. When the temperature is increased to 40°C, the SEM image (Figure 3b) reveals a more consolidated and cohesive microstructure. The surface seems smoother and more evenly coated in carbonate layers, suggesting a more efficient reaction. This confirms that carbonation is more efficient than at 40°C, with the presence of rhombohedral crystals, likely calcite, indicating more advanced carbonation. These observations align with the increased formation of siderite ($FeCO_3$) at this temperature, suggesting enhanced reactivity of iron-bearing phases and more diverse carbonate formation [11]. At 80°C (Figure 3c), the microstructure becomes solid and more tightly packed. The image shows extensive layers of calcium carbonate almost completely covering the particles, resulting in a smooth, uniform surface. EDX analysis confirms that the carbonate layers are primarily composed of calcium carbonate ($CaCO_3$), with calcium, carbon, and oxygen as the major elements. Higher temperatures accelerate the carbonation process, leading to more complete coverage and reduced porosity. The carbonate is almost fully integrated into the material, with minimal fractures. The formation of solid crystals, suggests highly effective carbonation at 80°C. EDX analysis of these solid crystals confirms their composition as calcite. At this temperature, the material becomes stronger and more stable due to the increased mineral reactions and crystal formation.

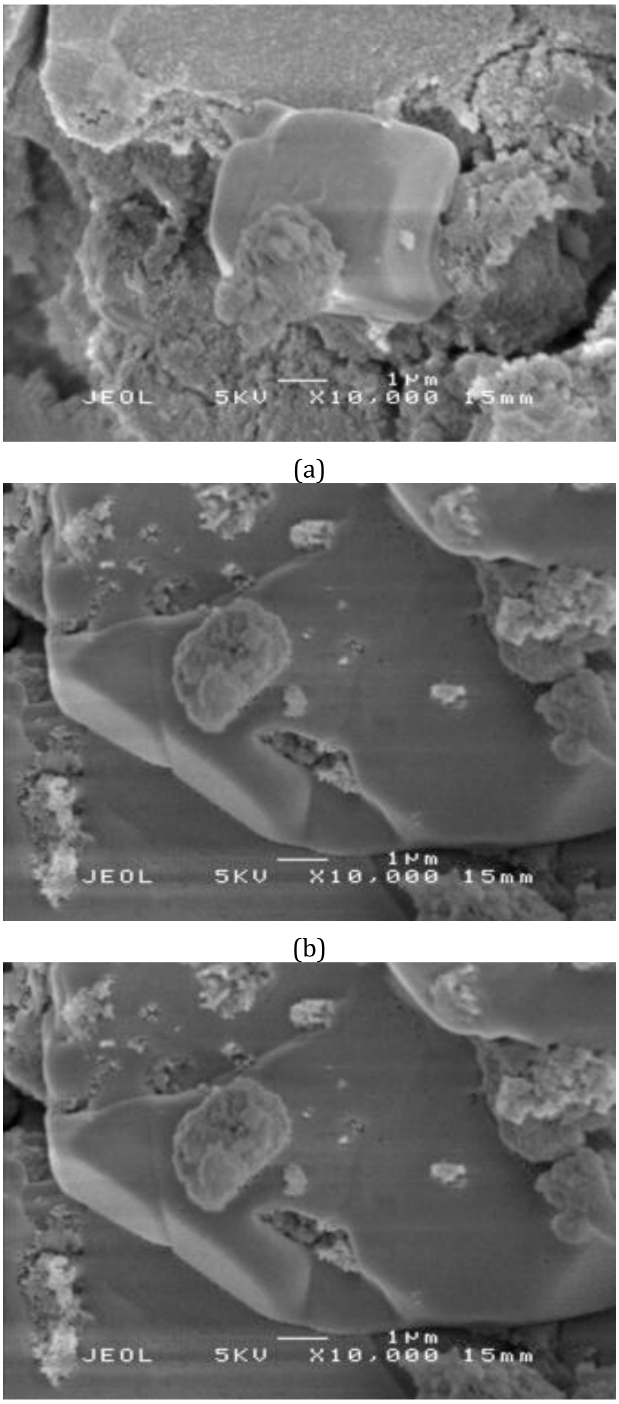

(a)

(b)

(c)

Fig. 3. SEM images of carbonated steel slag at different temperatures: (a) 25°C, (b) 40°C, and (c) 80°C, at ambient pressure (1 bar) and a reaction time of 60 minutes.

Supporting these observations, the oxide composition data (Table 1) from EDX analysis highlights a clear shift in oxide distribution with increasing temperature, which aligns with the SEM and EDX findings [12]. At 25°C, the total oxide content is 76.59%, dominated by CaO (26.93%), Fe_2O_3 (15.01%), and Na_2O (6.25%), indicating limited carbonation. As the temperature increases to 40°C, the total oxide content decreases slightly to 73.54%, with a notable decrease in CaO (19.60%) and an increase in Na_2O (35.75%), consistent with the formation of carbonate phases observed in SEM. At 80°C, the total oxide content further decreases to 68.38%, with CaO (12.03%) significantly consumed, as evidenced by the dense $CaCO_3$ layers in the SEM microstructure. Thus, the SEM and EDX analyses demonstrate that higher temperatures accelerate the carbonation process and enhance the formation of calcium carbonate. At 25°C, carbonation is limited to surface-level reactions, with a high concentration of unreacted calcium. At 40°C, carbonation becomes more uniform, with higher carbon content and the formation of both calcite and siderite. At 80°C, carbonation is nearly complete, with extensive carbonate formation and minimal fractures. These results highlight the importance of optimizing temperature to improve carbonate formation and carbonation efficiency.

Table 1. Oxide composition (%) of carbonated steel slag at different temperatures.

Oxide (%)	**Temperature**		
	25°C	**40°C**	**80°C**
Na_2O	6.25	35.75	41.57
MgO	4.72	1.21	2.01
Al_2O_3	-	5.90	5.44
SiO_2	14.59	5.28	3.72
CaO	26.93	19.60	12.03
MnO	1.12	-	-
Fe_2O_3	15.01	3.86	2.17
ZnO	7.95	1.94	1.43
Total	76.59	73.54	68.38

3.4. Thermogravimetric analysis

Figure 4 displays the TGA and DTG curves, demonstrating the impact of carbonation at three distinct temperatures (25°C, 40°C, and 80°C) on the thermal properties of both raw and carbonated steel slag. The carbonated samples exhibited significantly higher total weight loss, reaching a maximum of 36.71% at 25°C, which represents an 83.7% increase relative to the raw sample. At 40°C, the weight loss reduced to 32.82%, suggesting improved CO_2 retention as stable carbonates. At 80°C, the weight loss increased to 33.16%, indicating that the decomposition of other phases formed at elevated temperatures. The results align with the observations of [13], indicating that carbonation efficiency typically rises with temperature, although it may decline at higher temperatures due to lower CO_2 solubility and decreased diffusion rates of carbonate ions. Elevated temperatures generally promote the release of calcium ions, facilitating carbonation. This is evidenced by [14] who achieved up to 75% carbonation at 100°C under increased CO_2 pressures. Thus, the decreased CO_2 solubility at 80°C likely limited carbonation efficiency, indicating the complex connections between temperature and carbonation reactions. During the first thermal peak (30°C–150°C), which is linked to moisture loss, the raw steel slag demonstrates a relatively stable and minimal weight loss across all carbonation temperatures. In contrast, carbonated samples exhibit increasingly higher weight losses, with the most significant peak observed at 80°C and weight loss about 13.52%. The third thermal peak (600°C–800°C), indicative of calcium carbonate ($CaCO_3$) decomposition, is minimal in raw steel slag, thereby confirming its low carbonate content. Additionally, carbonation temperature can affect the particle size and morphology of the $CaCO_3$. Elevated temperatures may lead to the formation of larger or more crystalline particles, which could exhibit different thermal decomposition characteristics, resulting in a more pronounced peak during TGA/DTG analysis [15]. This suggests that the deeper decomposition peak observed at 80°C may be attributed to changes in the physical properties of the $CaCO_3$. Furthermore, the distribution of carbonate phases may vary with temperature. $CaCO_3$ may develop more efficiently than other carbonate phases, such magnesium carbonate ($MgCO_3$) or iron carbonate ($FeCO_3$), at greater carbonation temperatures. $CaCO_3$ in the TGA/DTG curves may indicate a more significant breakdown activity because of this selective formation. A more noticeable decomposition peak could arise from $CaCO_3$ produced at higher carbonation temperatures because of its increased thermal stability.

Findings indicate that carbonation significantly influences the properties of steel slag, resulting in notable differences between raw and carbonated samples. The findings suggests that although 25°C might encourage initial CO_2 absorption, achieving the full carbonation potential and stability of the formed carbonates can be more effectively accomplished at 40°C.

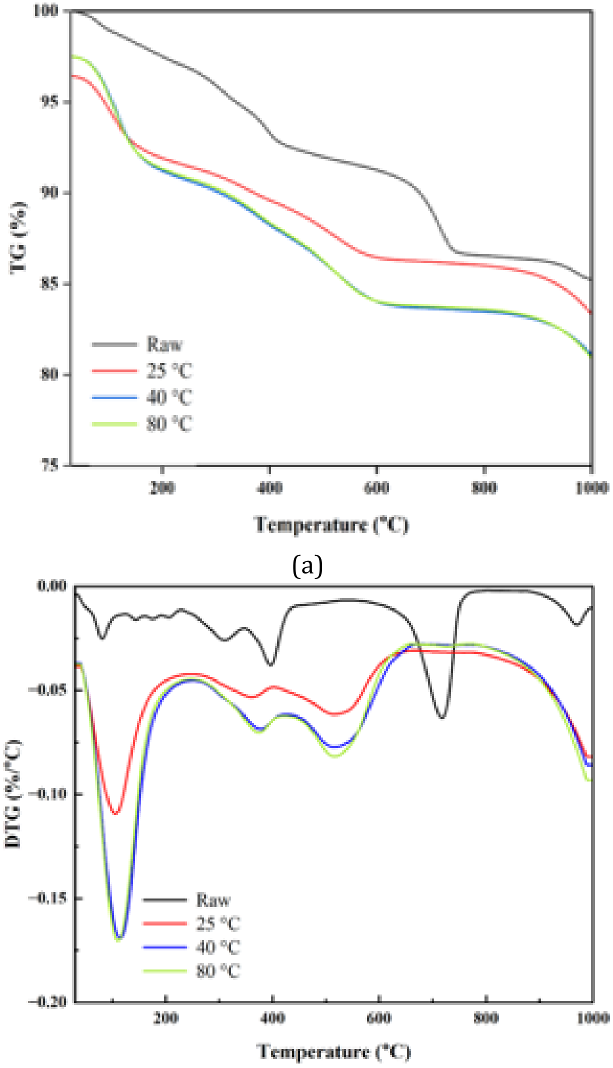

(a)

(b)

Fig. 4. (a) TGA and (b) DTG curves of carbonated steel slag at varying temperatures (25°C, 40°C, and 80°C).

4. CONCLUSION

This study demonstrates that carbonation of steel slag is significantly influenced by temperature, affecting both efficiency and the nature of carbonate products formed. The results indicate that a moderate temperature of 40°c is optimal for achieving efficient carbonation, offering a balance between enhanced reactivity and practical energy input. At this temperature, calcium and iron carbonate formation is notably improved, as evidenced by higher ca and fe carbonation efficiencies, mineralogical shifts toward calcite and siderite formation, and more consolidated microstructures observed in sem analysis. The edx and tga/dtg analyses further confirm these findings, showing substantial consumption of reactive oxides and higher co_2 retention in carbonated samples, especially at

40°c. Although carbonation at 80°c leads to extensive $CaCO_3$ formation and more uniform coverage, its energy demands and lower co_2 solubility suggest diminishing returns beyond the optimal point. Conversely, carbonation at 25°c is surface-limited and less efficient. Therefore, 40°c emerges as the most feasible temperature for maximizing carbonation efficiency and carbonate stability while minimizing energy input. These insights contribute to optimizing the mineral carbonation process for carbon capture and storage, particularly in valorizing industrial waste like steel slag as a viable co_2 sequestration medium.

Acknowledgement

The authors would like to acknowledge the laboratory staff of the Rikita Inouye Research Laboratory, Universiti Putra Malaysia (UPM) for technical assistance during the project. Special thanks are also extended to the laboratory staff of the Material Characterization Lab, UPM and Centre for Research and Instrumentation (CRIM), Universiti Kebangsaan Malaysia for their support in providing analytical assistance. Funding for the research was provided through the Fundamental Research

REFERENCES

[1] M. Aghaie, N. Rezaei, and S. Zendehboudi, "A systematic review on CO_2 capture with ionic liquids: Current status and future prospects," *Renew. Sustain. Energy Rev.*, vol. 96, pp. 502–525, 2018, doi: 10.1016/j.rser.2018.07.004.

[2] C.-H. Yu, C.-H. Huang, and C.-S. Tan, "A review of CO_2 capture by absorption and adsorption," *Aerosol Air Qual. Res.*, vol. 12, no. 5, pp. 745–769, 2012, doi: 10.4209/aaqr.2012.05.0132.

[3] A. Al-Mamoori, A. Krishnamurthy, A. A. Rownaghi, and F. Rezaei, "Carbon capture and utilization update," *Energy Technol.*, vol. 5, no. 6, pp. 834–849, 2017, doi: 10.1002/ente.201600747.

[4] M. M. F. Hasan, E. L. First, F. Boukouvala, and C. A. Floudas, "A multi-scale framework for CO_2 capture, utilization, and sequestration: CCUS and CCU," *Comput. Chem. Eng.*, vol. 81, pp. 2–21, 2015, doi: 10.1016/j.compchemeng.2015.04.034.

[5] J. Huang, Y. Fan, T. Liu, Y. Zhang, and P. Hu, "Carbon capture technology exploitation for vanadium tailings and assessment of CO_2 sequestration potential," *J. Environ. Manag.*, vol. 331, p. 117338, 2023, doi: 10.1016/j.jenvman.2023.117338.

[6] Z. Hou, J. Luo, Y. Xie, L. Wu, L. Huang, and Y. Xiong, "Carbon circular utilization and partially geological sequestration: Potentialities, challenges, and trends," *Energies*, vol. 16, no. 1, p. 324, 2023, doi: 10.3390/en16010324.

[7] M. H. Soomro, F. M. Kusin, F. Mohamat-Yusuff, and N. N. Nik Daud, "Elution of divalent cations from iron ore mining waste in an indirect aqueous mineral carbonation for carbon capture and storage," *Sustainability*, vol. 16, no. 2, p. 836, 2024, doi: 10.3390/su16020836.

[8] N. Li and C. Unluer, "Development of high-volume steel slag as cementitious material by ethylenediamine tetraacetic acid induced accelerated carbonation," *Powder Technol.*, vol. 428, p. 118899, 2023, doi: 10.1016/j.powtec.2023.118899.

[9] S. N. M. S. Hasan and F. M. Kusin, "Potential of mining waste from metallic mineral industry for carbon sequestration," *IOP Conf. Ser. Mater. Sci. Eng.*, vol. 458, p. 012013, 2018, doi: 10.1088/1757-899X/458/1/012013.

[10] Q. Song, M.-Z. Guo, L. Wang, and T.-C. Ling, "Use of steel slag as sustainable construction materials: A review of accelerated carbonation treatment," *Resour. Conserv. Recycl.*, vol. 173, p. 105740, 2021, doi: 10.1016/j.resconrec.2021.105740.

[11] A. Baras, J. Li, W. Ni, Z. Hussain, and M. Hitch, "Evaluation of potential factors affecting steel slag carbonation," *Processes*, vol. 11, no. 9, p. 2590, 2023, doi: 10.3390/pr11092590.

[12] D. Yuan et al., "High-temperature modification of steel slag using composite modifier containing silicon calcium slag, fly ash, and reservoir sediment," *Front. Earth Sci.*, vol. 11, 2023, doi: 10.3389/feart.2023.1214182.

[13] M. Tu, H. Zhao, Z. Lei, L. Wang, D. Chen, H. Yu, and T. Qi, "Aqueous carbonation of steel slag: A kinetics study," *ISIJ Int.*, vol. 55, no. 11, pp. 2509–2514, 2015, doi: 10.2355/isijinternational.ISIJINT-2015-142.

[14] F. Zhu et al., "Experimental investigation and mechanism analysis of direct aqueous mineral carbonation using steel slag," *Sustainability*, vol. 16, no. 1, p. 81, 2024.

[15] [15] Shimadzu Corporation, "Overview of analytical instruments," 2024. [Online]. Available: https://www.shimadzu.com/